International Journal of Biological Macromolecules 104 (2017) 43–55

Contents lists available at ScienceDirect

International Journal of Biological Macromolecules

journal homepage: www.elsevier.com/locate/ijbiomac

Cellulose nanocrystals from *Actinidia deliciosa* pruning residues combined with carvacrol in PVA_CH films with antioxidant/antimicrobial properties for packaging applications

Francesca Luzi[a], Elena Fortunati[a,*], Geremia Giovanale[b], Angelo Mazzaglia[b], Luigi Torre[a], Giorgio Mariano Balestra[b,*]

[a] University of Perugia, Civil Environmental Engineering Department, UdR INSTM, Strada di Pentima 4, 05100 Terni, Italy
[b] Department of Agricultural and Forestry Science (DAFNE), University of Tuscia, Via S. Camillo De Lellis snc, 01100 Viterbo, Italy

ARTICLE INFO

Article history:
Received 22 March 2017
Received in revised form 12 May 2017
Accepted 30 May 2017
Available online 3 June 2017

Keywords:
Kiwi pruning residues
Cellulose nanocrystals
Carvacrol
Nanocomposites
Antioxidant
Antibacterial
Plant pathogens
Active packaging

ABSTRACT

Kiwi *Actinidia deliciosa* pruning residues were here used for the first time as precursors for the extraction of high performing cellulose nanocrystals (CNC) by applying a bleaching treatment followed by an acidic hydrolysis. The resultant cellulosic nanostructures, obtained by an optimize extraction procedure (0.7% wt/v two times of sodium chlorite $NaClO_2$) followed by an hydrolysis step, were then used as reinforcements phases in poly(vinyl alcohol) (PVA) blended with natural chitosan (CH) based films and also combined, for the first time, with carvacrol used here as active agent. Morphological and optical characteristics, mechanical response, thermal and migration properties, moisture content and antioxidant and antimicrobial assays were conducted. The morphological, optical and colorimetric results underlined that no particular alterations were induced on the transparency and color of PVA and PVA_CH blend by the presence of CNC and carvacrol, while they were able to modulate the mechanical responses, to induce antioxidant activities maintaining the migration levels below the permitted limits and suggesting the possible application in industrial sectors. Finally, inhibitions on bacterial development were detected for multifunctional systems, suggesting their protective function against microorganisms contamination.

1. Introduction

New biodegradable multifunctional, antimicrobial and antioxidant systems were rapidly promoted and investigated in some different application fields and also in food packaging sector as valid eco-friendly possibility to improve the safety and quality of food products. In this scenario, bio-based and/or biodegradable polymers were considered to be a promising solution to reduce and/or limit the environmental impact respect to the traditional plastics [1,2]. The scientific community and the growing interest of humans promoted, in fact, the development of new edible and eco-friendly packaging considered as valid alternatives to reduce wastes and residues [3]. However, bio-based/biodegradable polymers are usually characterized by some restrictions in terms of properties respect to the traditional polymers, that could be addressed by using a nanotechnological approach [4–6].

In the last decade, researchers focused their attention on the use of lignocellulosic by-products as reinforcing fillers in polymeric matrices. The revalorization of lignocellulosic materials was largely investigated as a valid alternative to extract nanoreinforcements completely natural and renewable as cellulose nanofibers, cellulose nanocrystals (CNC) and/or nanolignin [4]. The main constituents of plant structure are: cellulose, hemicelluloses and lignin. Cellulose is the major structural component of plant cell walls, responsible for mechanical strength, hemicellulose macromolecules are often repeated polymers of pentoses and hexoses, while lignin forms a protective seal around the other two components i.e., cellulose and hemicelluloses [7,8]. Cellulosic nanostructures, as i.e., cellulose nanocrystals (CNC), can be recovered from different lignocellulosic wastes (or materials of scarce value) by carrying out applying two step treatments. A first step permits to remove and to clean the cellulosic materials from different components as lignin, hemicelluloses and pectin [9]; the second step consists in the removal of the amorphous components to obtain a high crystalline structure, also at the nanoscaled level, particular useful in a nanocomposite approach.

* Corresponding authors.
E-mail addresses: elena.fortunati@unipg.it (E. Fortunati), balestra@unitus.it (G.M. Balestra).

http://dx.doi.org/10.1016/j.ijbiomac.2017.05.176
0141-8130/

Every years, the plants need to be prune to increase their vigorous and splendor while, in the case of fruit plants, the prune is also necessary to improve the quality and the production of fruits. In Kiwi cultivation (*Actinidia deliciosa*) most of crop residues are produced by carrying out the usual pruning practice and the kiwi biomass produced annually by pruning was estimated to be of about 2.51 Mg DM ha^{-1} [10]. Moreover, the *Actinidia* cultivation, showed a growing trend and during the decade 2003–2012, the area under cultivation, excluding China, increased from just over 60,000 to almost 100,000 ha and Italy has become one of the world largest producer of kiwifruit [11].

In this research, the extraction of cellulose nanocrystals (CNC) from kiwi pruning stalks and their application in a nanocomposite approach was proposed for the first time. Nemli et al. previously investigated the suitability of kiwi (*Actinidia chinensis* Planch.) pruning as a raw material to use in the core layer of particleboards [12], while revalorization of pruning residuals from kiwi *Actinidia deliciosa* with and without bark was proposed by Gençer [13].

Here, CNC from kiwi pruning, were used, for the first time, as reinforcement phase in poly(vinyl alcohol) (PVA) and chitosan (CH) based blend. Cellulose nanocrystals are typically characterized by rigid rod monocrystalline domains with diameters ranging from 1 to 100 nm and the length from ten to hundreds of nm [14–18]. CH is a linear polysaccharide of randomly distributed β-(1–4)- linked D-glucosamine and *N*-acetyl-D-glucosamine, classified as Safe (GARS) by the US Food and Drug Administration (FDA) in 2001 [19–21]. CH is obtained from deacetylation of chitin; it is abundant in a variety of crustacean shells, such as crab shells, crawfish shells and shrimp shells [22]. In addition, chitosan presents bacteriostatic and fungistatic properties [23] that perfectly address the active packaging concept and the current trends and opinion regarding the need to inhibit pathogenic microbial activities in food products developing novel active/smart and intelligent packaging solutions [24]. Furthermore, with this objective, some different natural agents, essential oils and/or extracts, were recently involved in the production of biodegradable and eco-friendly packaging solutions [25–27] whereas carvacrol, an already studied antimicrobial additive in thermoplastic biodegradable based blends [28], was here considered as active ingredient and combined, for the first time, with CNC, in PVA_CH based films. Carvacrol is a phenolic compound extracted from oregano and thyme oil that possesses antioxidant and antimicrobial properties, and a particular aroma which makes it an attractive ingredient for certain types of foods [29–31].

In the present research, cellulose nanocrystals were extracted, for the first time of our knowledge, from kiwi pruning stalks by applying a bleaching treatment followed by an acidic hydrolysis and then used as reinforcement phases in water soluble polymers. Poly(vinyl alcohol) and chitosan (10%wt) were selected as polymer matrices while carvacrol was considered as antioxidant agent to improve the radical scavenging activities and antimicrobial response on the final produced packaging formulations. All produced PVA and PVA_10CH based systems were investigated in terms of optical, morphological, thermal and mechanical properties. Finally, functional characteristics of fundamental importance for food packaging sector in terms of antioxidant capacity, antimicrobial activity, overall migration and moisture content, were here deeply investigated to evaluate the effect of chitosan, carvacrol and cellulose nanocrystals on the final properties of PVA based systems.

2. Experimental part

2.1. Materials

Kiwi pruning wastes of *Actinidia deliciosa* were collected during winter pruning time from kiwifruit orchards in Central Italy, Lazio region (Cisterna di Latina, LT), the most important Italian kiwifruit area, where are cultivated around 8,000 ha of *Actinidia* spp.

All chemicals and reagents, including toluene, ethanol, sodium hydroxide (NaOH, reagent grade ≥98%), sodium chlorite ($NaClO_2$, puriss p.a. 80%), acetic acid (CH_3COOH) and sodium bisulfate ($NaHSO_4$, purum, anhydrous, 95.0%) were provided by Sigma-Aldrich® (Milan, Italy).

Polymer matrices, poly(vinyl alcohol) (PVA, average M_w 124–146 kg mol^{-1}, 99% hydrolyzed), and chitosan (CH) (viscosity: 200–800 cPs, degree of deacetylation:75-85%), were provided by Sigma-Aldrich® (Milan, Italy).

Carvacrol (Carv) with 98% purity was purchased from Sigma-Aldrich® (Milan, Italy) and it was selected as antimicrobial and antioxidant additive for the film formulations.

2.2. Chemical pre-treatment of kiwi pruning shoots

Kiwi pruning shoots (Fig. 1: Panel A-a and b) were firstly washed in distilled water several times (5 L of water for 150 g of wastes) in order to remove the powder and environmental contaminations. Subsequently, the pruning residues were treated for 72 h at room temperature (RT) with 1%w/v of NaOH solution (4 L for 150 g of wastes) and then for 2 h at 98 °C with 5%w/v of NaOH solution (2 L for 100 g) to remove the lignin components. The lignocellulosic materials were also mechanically retting and chopped in order to obtain individualized fibres (length around 10–15 mm). After the mechanical retting the fibres were dried at 60 °C for 24 h.

Furthermore, two different procedures were applied for the bleaching treatment in order to optimize this step. In the first case, the fibres were bleached one time with 5% wt/v of sodium chlorite ($NaClO_2$) (liquor ratio 1:50) while in the second case the fibres were treated two times with 0.7% wt/v of $NaClO_2$ (liquor ratio 1:50) [32]. The fibres during both the procedures were boiled for two hours and the solution pH was 4 by means acetic acid. At the end of bleaching treatments the materials were washed several times and treated with sodium bisulphate solution at 5% wt/v for 30 min at RT (liquor ratio 1:40), washed again with deionized water, treated with NaOH solution at 17.5% wt/v for 20 min at RT (liquor ratio 1:50) and then finally dried at 60 °C for 24 h.

2.3. Cellulose nanocrystal extraction

Cellulose nanocrystals (CNC) were prepared from bleached kiwi stalks (treated at both 5% wt/v or 0.7% wt/v of sodium chlorite $NaClO_2$) by means of acid hydrolysis (64% (wt/wt) sulphuric acid at 45 °C for 30 min) [33,34]. Cellulose suspension was centrifuged and dialyzed, prior to its addition for 48 h to a mixed bed ion exchange resin (Dowex Marathon MR-3 hydrogen and hydroxide form). The resultant cellulose nanocrystal aqueous suspension was ultrasonicated by means of a tip sonicator (Vibracell, 750) for 5 min. For both the applied procedures the final yield was calculated as% of initial weight of the used raw material.

2.4. Characterization of raw materials, bleached fibres and extracted cellulose nanocrystals

The morphological structure of kiwi pruning residues, pre-treated stalks and extracted cellulose nanocrystals were investigated by field emission scanning electron microscope (FESEM, Supra 25-Zeiss). The pruning, pre-treated and hydrolyzed materials were prepared following the procedure described by Fortunati and co-authors [35].

X-ray diffraction patterns of cellulose nanocrystals, obtained by means of the acidic hydrolysis of cellulosic materials bleached applying the two different pre-treatments (5% wt/v or 0.7% wt/v of sodium chlorite), were collected with a PANalytical X'PERT PRO

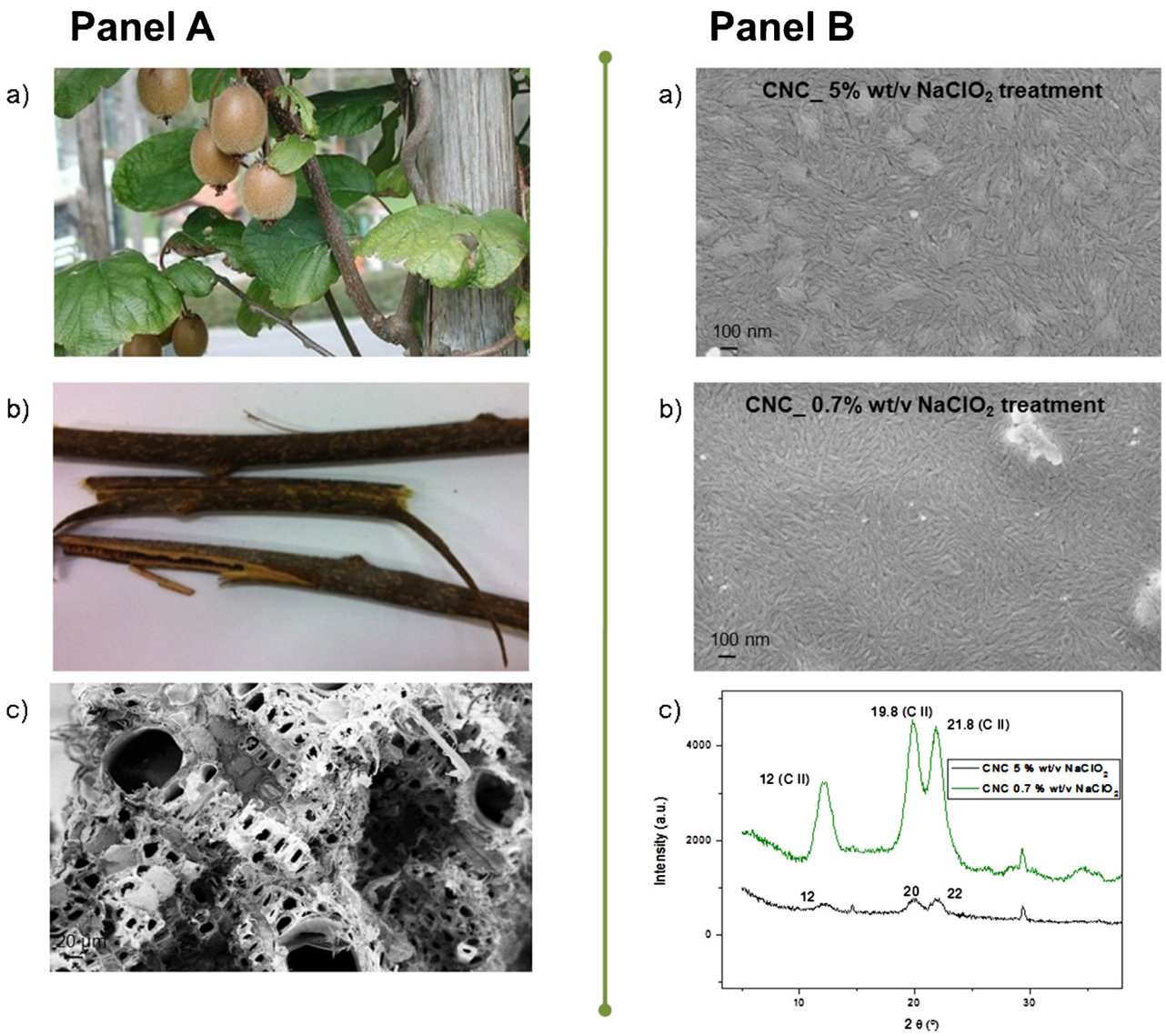

Fig. 1. Panel A: Visual image of Kiwi tree (a), visual image of pruned kiwi shoots (b) and FESEM of kiwi shoot fractured surfaces (c). Panel B: FESEM investigation of CNC extracted from pre-treated kiwi fibres with 5% wt/v of sodium chlorite (a) and with 0.7% wt/v of sodium chlorite (b). X-ray diffraction (XRD) patterns of CNC extracted by applying two different bleaching treatments.

diffractometer source Cu K a k = 1.54184 Å, 40 kV e 40 mA supply, PW3050 goniometer and X'Celerator fast detector using a 0017° 2theta step and 200 s counting time per each step.

Fourier infrared (FTIR) spectra of raw, chemically pre-treated pruning wastes were analyzed by using a Jasco FTIR 615 spectrometer in the 400–4.000 cm^{-1} range, in transmission mode. The cellulosic materials were analyzed by means of KBr discs made by using pulverized fibres and CNC and dust of KBr.

Finally, thermogravimetric measurements (TGA) were performed by using a Seiko Exstar 6300. The analysis used and heating scan from 30 to 900 °C at 10 °C min^{-1} in nitrogen atmosphere.

2.5. Production of PVA_CH based systems

PVA and PVA_CH based films were prepared by solvent casting method by using the procedure described by Fortunati et al. [20]. Initially, PVA and PVA_CH based films were prepared dissolving the polymer in deionized water at 5% (wt/v) under magnetic stirring at 90 °C for 4 h, while chitosan (0.15% (wt/wt)) polymer was dissolved in water with glacial acetic acid (1% (v/v)) under magnetic stirring at 40 °C for 12 h. PVA_CH blend films were produced mixing CH in solution (10% wt respect to the weight of PVA) with PVA polymer (90% wt), the obtained blend solution was then sonicated for 5 min at 40% of amplitude. The polymeric solution was cast onto a Petri dish cover by a *Teflon*® and dried in an oven at 40 °C for 24–48 h. PVA_CH based nanocomposites reinforced with CNC were prepared adding 3% wt of cellulose nanocrystals to homogeneous polymeric blend solution sonicated for 2 min at 40% of amplitude. PVA and PVA_CH based active films were also produced loading the different formulations with 5%wt of carvacrol. Before to prepare PVA_5Carv, PVA_10CH_Carv and PVA_10CH_5Carv_3CNC films, carvacrol aqueous solution was prepared by mixing the active principle with deionized water under mechanical stirring for 1 h at RT and homogenized in a sonic bath for 1 h at RT and then added to polymer solution. PVA and PVA_CH based films loaded with 5% wt of carvacrol were mixed by magnetic stirrer for 1 h at RT and then cast onto Petri dish and dried in an oven at 40 °C for 24–48 h. The films (of 90 mm diameter and 50 ± 5 μm thick) were equilibrated after the processing in desiccators at 25 °C and around 20 RH% by using a silica gel granular (Sigma–Aldrich®). Table 1 summarizes

Table 1
Material formulations.

Formulations	PVA (% wt)	CH (% wt)	Carv (% wt)	CNC (% wt)
PVA	100	–	–	–
PVA_10CH	90	10	–	–
PVA_5Carv	95	–	5	–
PVA_10CH_5Carv	85	10	5	–
PVA_10CH_3CNC	87	10	–	3
PVA_5Carv_3CNC	92	–	5	3
PVA_10CH_5Carv_3CNC	82	10	5	3

the compositions of all produced formulations, in terms of chitosan, carvacrol and cellulose nanocrystals content respect to PVA matrix.

2.6. Characterization of PVA_CH based films

2.6.1. Morphology, transparency and colour analysis

The microstructure of PVA and PVA_CH fractured surfaces were investigated by FESEM (Supra 25-Zeiss) after gold sputtering and by using an accelerating voltage of 5 kV.

The transparency of different formulations were investigated by UV–vis spectroscopy in the range 250–900 nm by using a Perkin Elmer Lambda 35.

Colour changes of PVA films due to the presence of chitosan, carvacrol and CNC were analyzed by means of a spectrophotometer (CM-2300d Konica Minolta, Japan). Data were investigated by using the SCI 10/D65 method whereas CIELAB colour variables, as defined by the Commission Internationale de l'Éclairage (CIE 1995), were used. The different produced formulations were positioned on a white standard substrate and L^*, a^*, and b^* parameters were determined. L^* value ranges from 0 (black) to 100 (white); a^* value ranges from −80 (green) to 100 (red); and b^* value ranges from −80 (blue) to 70 (yellow). Samples were analyzed in triplicate, and three measurements were taken at random locations on each of the studied films. The total colour difference ΔE^* between PVA and PVA_CH based formulations and it was obtained as indicated in Eq. (1).

$$\Delta E^* = \sqrt{(\Delta L^*)^2 + (\Delta a^*)^2 + (\Delta b^*)^2} \quad (1)$$

Gloss value was also determined by using the SCI 10/D65.

2.6.2. Thermal characterizations

Thermal characterization of neat PVA and PVA_CH based formulations was performed by differential scanning calorimetric (DSC) on a TA Instruments DSC Q200 (TA Instruments Inc., USA) under nitrogen atmosphere in the range from −25 to 240 °C at 10 °C min^{-1}, carrying out two heating and one cooling scan. The glass transition temperature (T_g) was investigated during both heating and cooling scan; the melting temperature and enthalpy (T_m and ΔH_m) were determined from the second heating scan, whereas crystallization temperature and enthalpy (T_c and ΔH_c) were determined from the cooling scan. The crystallinity degree was evaluated according to Eq. (2):

$$\chi = \frac{1}{(1 - m_f)} \left[\frac{\Delta H}{\Delta H_0}\right] * 100 \quad (2)$$

where ΔH is the enthalpy for melting or crystallization; ΔH_0 is enthalpy of melting for a 100% crystalline PVA sample, taken as 161.6 J g^{-1} [36] and (1-m_f) is the weight fraction of PVA in the sample.

Thermogravimetric measurements (TGA) were performed by using a Seiko Exstar 6300. Heating scans from 30 to 600 °C at 10 °C min^{-1} under nitrogen atmosphere were performed for each sample.

2.6.3. Mechanical characterization

The mechanical properties of neat PVA and PVA_CH based films were evaluated by tensile tests, by using rectangular probes (50 mm × 10 mm) on the basis of UNI ISO 527 standard with a load cell of 500 N, an initial gauge length of 25 mm and a crosshead speed of 50 mm min^{-1}. The tensile strength (σ_B), elongation at break (ε_B) and the Young's modulus (E), were calculated from the stress-strain curves. The analysis were carried out at room temperature and five samples were tested.

2.6.4. Antiradical activity

The radical scavenging activity of PVA and PVA_CH based systems was determined by using a spectroscopic method according to the procedure proposed in literature by Byun et al. [37]. The different PVA and PVA_CH based films (0.1 g) were cut into small pieces and immersed in 2 mL of methanol for 24 h at RT. An aliquot of methanol extract (1 mL) was mixed with 1 mL of DPPH in methanol (50 mg/L^{-1}). The mixture was allowed to stand at room temperature in the dark for 60 min. The absorbance was measured at 517 nm using a UV spectrometer (Varian (Cary 4000, USA) ultraviolet-visible (UV–vis) spectrophotometer). The mixture solution of methanol extracted from neat PVA and DPPH methanol was used as control. DPPH radical scavenging activity (*RSA*) was calculated according to Eq. (3):

$$RSA(\%) = \frac{A_{Control} - A_{Sample}}{A_{Control}} * 100 \quad (3)$$

where A_{sample} is the absorbance of sample and $A_{control}$ is the absorbance of the control.

2.6.5. Overall migration and moisture content

The overall migration analysis of neat PVA, PVA_CH blend films and was determined in triplicate in simulant A (10% (v/v) ethanol water solution) and simulant D (isooctane) according to Commission Regulation (EU) No 10/2011. The samples of 10 cm^2 were immersed in 10 mL of simulant [38]. Samples were maintained at 40 °C for 10 days according to EN-1186 standard (European Standard EN 1186-1: 2002) in contact with the stimulant A, while in the case of simulate D the samples were maintained in contact for 2 days at 20 °C. The simulant was then evaporated and residues weighed with an analytical balance (Sartorius ATILON) with ±0.01 mg precision. The migrated materials were expressed in mg kg^{-1} of the/each simulant.

The moisture content of produced films (MC), equilibrated at 53% RH and 25 °C, was analyzed by drying the samples in a vacuum oven at 40 °C for 72 h. Later on, the pre-dried samples were placed in desiccators containing $Mg(NO_3)_2$ until reaching constant weight. Three replicates per film formulation for 1 and 5 weeks were analyzed.

2.6.6. Antibacterial analysis

Four known high virulent plant pathogenic bacterial strains, *Pectobcterium carotovorum* susp. *odoriferum* (Pco – CFBP 1878T), *Erwinia amylovora* (Ea – CFBP 1430), *Xanthomonas axonopodis* pv. *vesicatoria* (Xav – CFBP 3274), and *Xanthomonas arboricola* pv. *pruni* (Xap – CFBP 3894) were here considered for films antimicrobial assays. Pco results able to cause severe soft rots on several vegetable species; Ea, Xap and Xav are quarantine pests particularly dangerous in and out of EU respect to a huge number of cultivated fruit and vegetable plant species [39,40]. For each bacterial strain, by means of a turbidimeter (Biolog Turbidimeter Model 21907), it is proceeded to the reading of the optical density of the bacterial suspension to a wavelength equal to 590 nm. This reading allowed to make appropriate dilutions with sterile distilled water necessary to obtain, for each bacterial suspension per isolate, a concentration of 1 × 10^8 colonies forming units CFU/mL. The reading of the optical

density was different for the strains; in fact it was of 0.22 nm for Xav, 0.24 nm for Xap, 0.20 nm for Ea and of 0.18 nm for Pco, respectively. These values were determined by the development of the calibration curve, previously performed the start of the tests. The bacterial suspension at a concentration of 1×10^8 CFU/mL 1 mL was 1/10 diluted with sterile distilled water (SDW) in order to obtain a bacterial concentration of 1×10^7 CFU/mL. Since this was then taken 1 mL and pipetted into a sterile falcon, which were present in 9 mL of NB 32% so as to obtain a suspension of 10 mL to bacterial concentration of 1×10^6 CFU/mL. The 8 sterile falcon had been previously prepared with 9 mL of NB 32% which was immersed in a film of dimensions of 1 cm × 1 cm. Only one of the falcon object of the tests was devoid of the film, as this had positive control function. The bacterial solutions at a concentration of 1×10^6 CFU/mL were incubated in the agitator-orbital incubator at a temperature of $27 \pm 1^\circ$ C at 150 g min^{-1}. Subsequently they were performed levies after 1 h, 3 h, 12 h, 24 h after incubation. For each sample was taken 1 mL suspension for thesis and then were carried out its decimal dilutions. For each 100 μL dilution carried out they were pipetted into a Petri dish containing the growing media. The plates were then incubated in the thermostat for 24–48 h at a temperature of $27 \pm 1^\circ$ C, subsequently to which they proceeded to the count of the bacterial developed colonies.

3. Results and discussion

3.1. Optimization of bleaching treatment for the extraction of cellulose nanocrystals

The pruning from kiwi plants generate an abundant, renewable, lignocellulosic residue, which is usually burned in the field to prevent the propagation of vegetal diseases which could incur economic costs and environmental concerns. Kiwi residues of any type must be taken out of the field, because dead and dry residues host disease and insects. For this reason, kiwi pruning should be converted to more beneficial products. Moreover, the chemical composition of kiwi (*Actinidia deliciosa*) wood was previously determined according to the standard TAPPI methods that has attested a high amount of holocellulose (73.50%), α-cellulose of 38.30% and 25.30% of lignin [13]. It is possible to notice that the holocellulose content of the kiwi is approximately equal to that of the hardwoods, which indicates that kiwi should give a fairly high yield of pulp when properly treated. For this reason, kiwi pruning were here considered as raw materials for the extraction of high performing cellulose nanocrystals to use as reinforcement phases in biodegradable based film formulations. The morphology of kiwi pruning stalks (Fig. 1: Panel A-a and b), used here as raw materials, was shown in Fig. 1: Panel A-c. Kiwi stalks have a heterogeneous structure characterized by an external lignocellulosic wall and an interior void core. FESEM image shows the porous like-honeycomb network that characterizes the cross section of kiwi stalks [41]. Both the applied bleaching treatments (at 5% wt/v or 0.7% wt/v of sodium chlorite) provoked an evident defibrillation process of the stalks (data not shown) and a whiting process as a consequence of hemicellulose and lignin removal as previous observed for other agricultural residues [35]. The bleached fibres were then hydrolysed and the morphologies of the resultant cellulose nanocrystals, are reported in Fig. 1: Panel B-a and b, for the pre-treatment at 5% wt/v and 0.7% wt/v with the sodium chlorite, respectively. The FESEM images confirm that the aqueous suspensions contained cellulose nanocrystals consisted mostly of individual crystals with the previously reported acicular structure ranged from 100 to 150 nm in length and 10–15 nm in diameter [42]; however, FESEM image for the CNC extracted after the pre-treatment at 5% wt/v of sodium chlorite (Fig. 1: Panel B-a) shows the presence of more evident unreacted residues that quite disappeared completely with the second applied procedure (0.7% wt/v of sodium chlorite). The presence of these residues underlined the inefficacy of the first applied treatment and this evidence was also confirmed by the calculation of the yield. A reaction efficiency of 3% was, in fact, obtained by applying 5% wt/v of sodium chlorite whereas a yield of ca. 14% was measured for the bleaching treatment (0.7% wt/v two times of sodium chlorite $NaClO_2$).

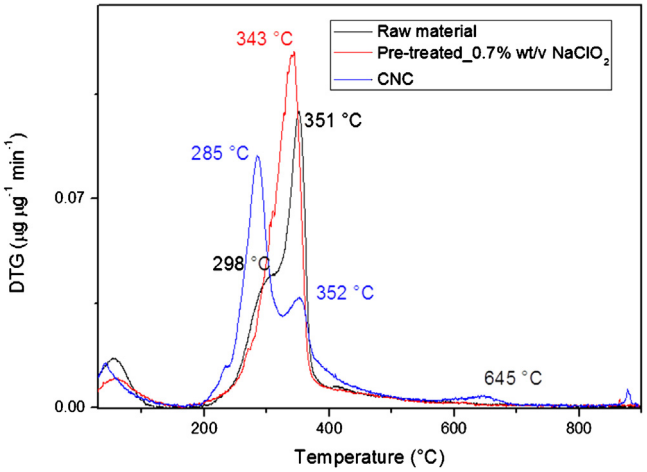

Fig. 2. Derivative curves (DTG) of raw, pre-treated and CNC from kiwi pruning residues.

XRD studies were done on both type of cellulose nanocrystals extracted after the two different bleaching treatments to investigate the effect of chemical purification on the crystallinity patterns of the obtained materials. Fig. 1: Panel B-c shows the X-ray diffraction peaks for CNC extracted after a 5% wt/v or 0.7% wt/v treatment with sodium chlorite. In its native state, cellulose usually shows a semicrystalline structure with crystalline domains of cellulose I with parallel chains connected side-by-side via hydrogen bonding in flat sheets embedded in an amorphous phase made by lignin and hemicellulose. Regeneration and mercerization of cellulose based materials induce a transformation from cellulose I structure to cellulose II, where the chains are stacked to form corrugated sheets bounded together by a hydrogen bonding network. Both XRD patterns for different CNC showed the characteristic diffraction features of cellulose II crystalline domains [43], although lower intensities of all the peaks were registered for CNC extracted after the bleaching at 5% wt/v respect to the bleaching at 0.7% wt/v with sodium chlorite.

On the base of previous discussed results, CNC extracted applying two 0.7% wt/v treatments with sodium chlorite, were selected as reinforcement phases in PVA_CH based film formulations. Before nanocomposite production and characterization, thermal investigations of raw material, pre-treated fibres (two times 0.7% wt/v with $NaClO_2$) and resultant CNC were performed by TGA and the results in terms of weight loss derivative are summarized in Fig. 2. The DTG curves (Fig. 2) suggest that the pyrolysis process of kiwi stalks can be separated into three main stages: the first weight loss is due to moisture loss, the second is due to the main thermal decomposition of cellulose (centered at 351 °C with a shoulder peak at 298 °C due to hemicellulose and lignin components) [44,45] and the third step (over 600 °C) is related to the lignin and hemicellulose decomposition. In the case of pre-treated fibres, the first weight loss was reduced, while the elimination of the shoulder in the second peak of the DTG profile confirmed the elimination of hemicellulose and lignin material by the treatment with sodium hydroxide. In the case of CNC, two well-separated pyrolysis processes are observed in the DTG curves. The first main signal is likely due to the weaker

interaction of single bond OH groups in cellulose that requires less energy to start the thermal degradation process, while the second DTG peak of the cellulose remain centered at 352 °C [46].

3.2. Morphological investigation, transparency and colorimetric analyses of PVA and PVA_CH based systems

Fig. 3 shows the microstructure of the cross-section surfaces of PVA based films, analyzed by FESEM. The FESEM investigation was carried out to evaluate the effect of chitosan, carvacrol and cellulose nanocrystals on the microstructure of PVA and PVA_CH based systems. PVA film fractured surface appeared homogeneous, smooth and uniform (Fig. 3a) [47,48] as typical for a thermoplastic semi-crystalline polymers [25]. This behavior highlighted the good processability and film-forming properties of PVA during solvent casting process [25,42]. A similar microstructure was also revealed for PVA_CH based films: the cross sections of the blend appeared, in fact, homogeneous and uniform without the presence of cracks, phase separations, droplets or irregularities (Fig. 3b) [20,25,47] underlining the good interaction and compatibility of the two selected polymeric matrices [49]. Furthermore, the presence of carvacrol in PVA_5Carv and in PVA_10CH_5Carv films (Fig. 3c,d) and the addition of also cellulose nanocrystals in PVA_10CH_3CNC, PVA_5Carv_3CNC and PVA_10CH_5Carv_3CNC (Fig. 3e–g) did not provoke particular alterations of the PVA and PVA_CH fractured surfaces. The aspect of the all produced formulations reinforced with cellulose nanocrystals was homogeneous, wavy and without the presence of CNC agglomerates (Fig. 3e–g) highlighting the good interaction between the cellulosic nanofiller and the polymer matrices obtained during the film processing [20,36].

The visual appearance and the color of a material produced for packaging is one of the most important quality and property in the market sector and it can influence the commercial success and the choice of consumer acceptance of the different products. Visual observation and transparency properties from the transmittance UV–vis measurements of PVA and PVA_CH based films were shown in Fig. 4a,b. Fig. 4a shows, as an example, the appearance of PVA_10CH_5Carv_3CNC based nanocomposite underlining that the transparency of the original PVA matrix was maintained, after the processing, also when both carvacrol and CNC at 3% wt, were added to PVA_CH blend. PVA, as shown in Fig. 4b, is a transparent polymer (transmittance of 94.2% at a visible wavelength of 600 nm), however the presence of chitosan, carvacrol and CNC did not influence the transparency values detected at 600 nm (Fig. 4b). All the produced systems maintained good levels of transparency (85%) from 450 to 900 nm, due to the absence of aggregates, the high homogeneity and compatibility of both polymeric matrices, and the good dispersion of CNC into PVA or PVA_CH blend as observed by FESEM investigation (Fig. 3). However, the transparency values decreased progressively reducing the wavelength (in the range 250–450 nm). At 280 nm the reduction of the transmittance of PVA_10CH based films was due to the presence of chitosan in the PVA matrix. This behavior was related to the color of chitosan and in particular to the presence of double bonds, particularly those of C=O [49–51].

The color and gloss parameters of PVA based formulations were shown in Table 2. The colorimetric and gloss analysis were performed to investigate the influence of the chitosan, carvacrol and CNC on the PVA optical properties. PVA film was characterized by high lightness value ($L^* = 99.09 \pm 0.06$) and no significant variations were registered for the different PVA based systems as for a^* coordinates. Positive values were registered for b^* parameter, indicating a slight deviation towards yellow induced by the color of both chitosan and carvacrol and in accord also with UV–vis analysis results (Fig. 4b). PVA_10CH_5Carv_3CNC showed the highest values of b^* coordinate and also, as consequence, the highest ΔE^* variation respect to PVA. The increase in b^* parameter and the reduction of transmittance of different produced films were considered helpful to reduce oxidative deterioration in packaged foodstuffs [51]. The colour differences ΔE^* were evaluated between the PVA and all the other produced systems. The highest ΔE^* value was estimated for PVA_10CH_5Carv_3CNC based system ($\Delta E^* = 1.66$) but, since $\Delta E^* = 2$ is the limit for the human eye perception [35,52], the presence of chitosan, carvacrol and/or CNC did not evidently compromise the color of the produced formulations respect to the PVA matrix.

The gloss values of PVA and PVA based formulations were summarized in Table 2 and no particular differences were observed among the different produced formulations due to the good compatibility and interactions of PVA with chitosan as previously observed by Bonilla et al. [49] and the good distribution of carvacrol and CNC obtained during the processing and just proved by previous characterizations. PVA film was characterized by a gloss value of $(234 \pm 3)^\circ$, and a slight increase was only registered for PVA_10CH_5Carv_3CNC (gloss value of $(242 \pm 4)^\circ$).

3.3. Thermal and mechanical characterizations of PVA and PVA_CH based systems

Thermal properties of PVA and PVA_CH based systems were investigated by differential scanning calorimetry (DSC) and thermogravimetric analysis (TGA) in order to evaluate the effect of chitosan, carvacrol and cellulose nanocrystals in PVA films. The results are shown in Table 3 while the derivative curves of the mass loss (DTG) are reported in Fig. 5a.

DSC thermal properties of PVA and PVA_CH based formulations were obtained by the cooling and second heating scans (Table 3) to investigate the glass transition temperature, crystallization and melting phenomena. A slight increase of glass transition temperature (T_g) (of about 3 °C with the presence of CH and/or carvacrol and of about 4–5 °C when also CNC were introduced) was revealed during both the cooling and the second heating scans [20]. Moreover, during the cooling scan, the addition of CH in PVA based films determined a decrease of the crystallization enthalpy [52] and, as consequence, a reduction of the crystallinity degree (X_c) due to the amorphous nature of chitosan. The addition of CH in PVA film determined also a shift to lower temperature of about 15 °C of the crystallization temperature (T_c) respect to PVA film (PVA: $T_c = 191.3 \pm 0.8$ °C and PVA_10CH: $T_c = 177.5 \pm 0.8$ °C). The presence of carvacrol in PVA and in PVA_10CH systems (PVA_5Carv and PVA_10CH_5Carv) did not affect the crystallization temperature (T_c) and the crystallization enthalpy (ΔH_c) respect to PVA and PVA_10CH films, and a similar result was also obtained after the addition of CNC to PVA_10CH, PVA_5Carv and PVA_10CH_5Carv film.

During the second heating scan, the addition of carvacrol in PVA film (PVA_5Carv) determined an increase of ΔH_m around 4 J/g (PVA: $\Delta H_m = 33.0 \pm 0.9$ J/g and PVA_5Carv: $\Delta H_m = 37.2 \pm 1.6$ J/g). An increase of ΔH_m was also registered adding CNC in PVA_5Carv as a consequence of nucleation effect induced by the presence of the nanoreinforcements [54]. In the case of PVA_10CH based systems the addition of CNC induced a slight decrease of melting enthalpy (ΔH_m) of PVA_10CH_3CNC and PVA_10CH_5Carv_3CNC respect to PVA_10CH and PVA_10CH_5Carv, respectively. This behavior determined a reduction of crystallinity degree measured during the second heating scan (X_m). The typical nucleation phenomenon induced by CNC in thermoplastic matrices [41,54] and also here reported for PVA based formulations, it was not so evident when CNC were added to PVA_CH since the presence of chitosan, with its amorphous nature [53], was predominant in the thermal response of produced PVA_CH based formulations [20].

The thermal degradative properties of PVA and PVA_10CH based systems were investigated by TGA under nitrogen atmosphere in order to evaluate the effect of CH, Carv and CNC on their degradative properties. The maximum degradation temperatures (T_{max}) of

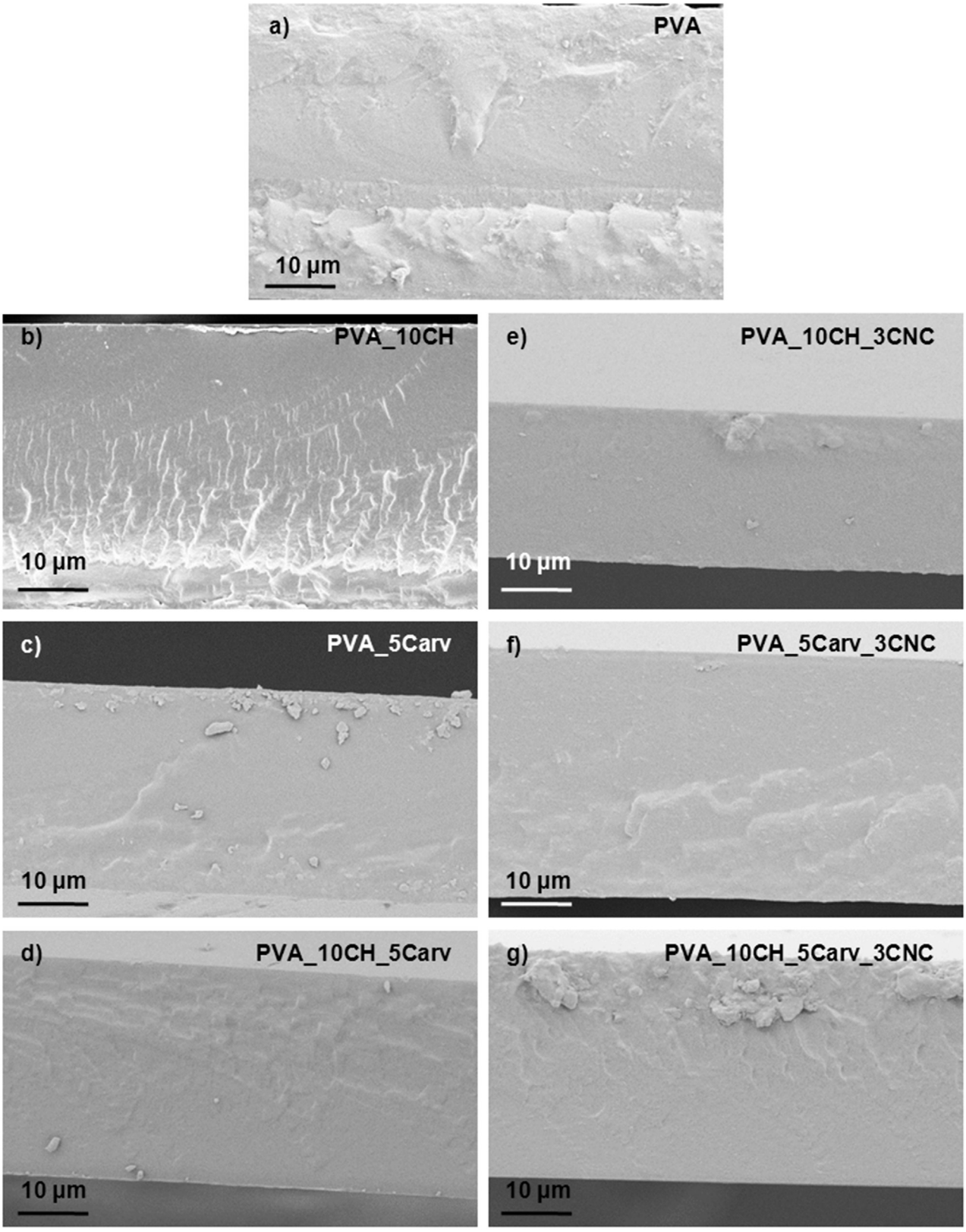

Fig. 3. FESEM investigation of fractured surface of PVA based formulations.

different formulations was summarized in Table 3 while the derivative curves of the mass loss (DTG) are shown in Fig. 5a. PVA and PVA_10CH based formulations were characterized by a multi-step degradation behavior. The first step of degradation was centered at low temperature around 80–110 °C and corresponded to the moisture evaporation and to the weight loss of low molecular weight compounds [26,42,55]. The second peak, centered at around 170 °C, was present only in the PVA_10CH based formulations and it was

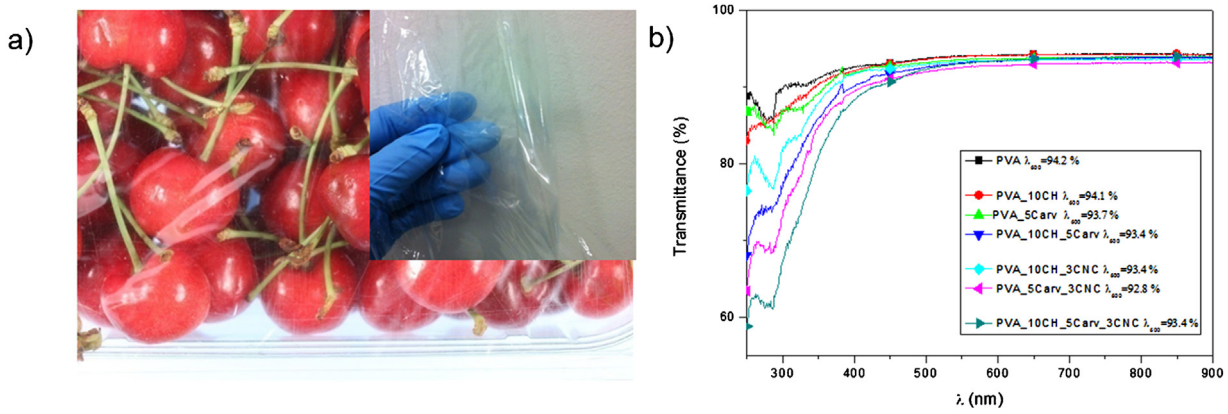

Fig. 4. Visual image of PVA_10CH_5Carv_3CNC system (a). UV–vis analysis of PVA based formulation.

Table 2
Colour coordinates of PVA based systems.

Formulations	L*	a*	b*	ΔE*	Gloss (°)
PVA	99.09 ± 0.06	−0.10 ± 0.01	0.16 ± 0.02	–	234 ± 3
PVA_10CH	98.81 ± 0.08	−0.22 ± 0.03	1.04 ± 0.15	0.93	232 ± 1
PVA_5Carv	99.12 ± 0.01	−0.08 ± 0.01	0.28 ± 0.01	0.13	227 ± 4
PVA_10CH_5Carv	98.43 ± 0.15	−0.21 ± 0.01	1.20 ± 0.16	0.70	228 ± 6
PVA_10CH_3CNC	98.49 ± 0.05	−0.23 ± 0.01	1.42 ± 0.08	1.40	232 ± 3
PVA_5Carv_3CNC	98.65 ± 0.01	−0.11 ± 0.01	0.61 ± 0.06	0.63	231 ± 2
PVA_10CH_5Carv_3CNC	98.26 ± 0.09	−0.24 ± 0.02	1.60 ± 0.20	1.66	242 ± 4

Table 3
DSC and TGA data of PVA based systems.

Formulations	DSC								TGA
	Cooling scan				Second heating scan				
	T_g (°C)	ΔH_c(J/g)	T_c (°C)	X_c (%)	T_g (°C)	ΔH_m (J/g)	T_m (°C)	X_m (%)	T_{max} (°C)
PVA	72.8 ± 0.7	40.6 ± 2.8	191.3 ± 0.8	25.1 ± 1.7	79.6 ± 0.0	33.0 ± 0.9	216.9 ± 0.7	20.4 ± 0.6	257 ± 1
PVA_10CH	75.3 ± 0.2	28.9 ± 1.7	177.5 ± 0.8	16.1 ± 0.9	82.9 ± 0.7	34.3 ± 0.6	212.1 ± 0.9	19.1 ± 0.3	265 ± 1
PVA_5Carv	75.5 ± 0.1	44.9 ± 0.3	189.1 ± 2.1	26.4 ± 0.2	79.7 ± 1.4	37.2 ± 1.6	217.0 ± 1.6	21.9 ± 0.9	259 ± 2
PVA_10CH_5Carv	74.9 ± 0.5	32.2 ± 3.1	179.4 ± 1.4	17.0 ± 1.6	81.4 ± 0.3	30.6 ± 3.4	214.4 ± 1.8	16.9 ± 1.9	267 ± 3
PVA_10CH_3CNC	76.2 ± 0.4	28.6 ± 0.6	175.3 ± 0.6	15.4 ± 0.3	81.9 ± 0.7	25.0 ± 0.9	210.0 ± 1.2	13.5 ± 0.47	257 ± 1
PVA_5Carv_3CNC	78.1 ± 0.5	45.5 ± 1.1	189.3 ± 0.5	25.9 ± 0.6	79.6 ± 1.3	40.9 ± 2.8	215.1 ± 0.2	23.3 ± 1.6	261 ± 1
PVA_10CH_5Carv_3CNC	75.1 ± 1.5	34.9 ± 0.4	177.5 ± 0.4	17.7 ± 0.2	78.8 ± 0.1	22.42 ± 0.1	212.0 ± 0.1	11.4 ± 0.1	261 ± 2

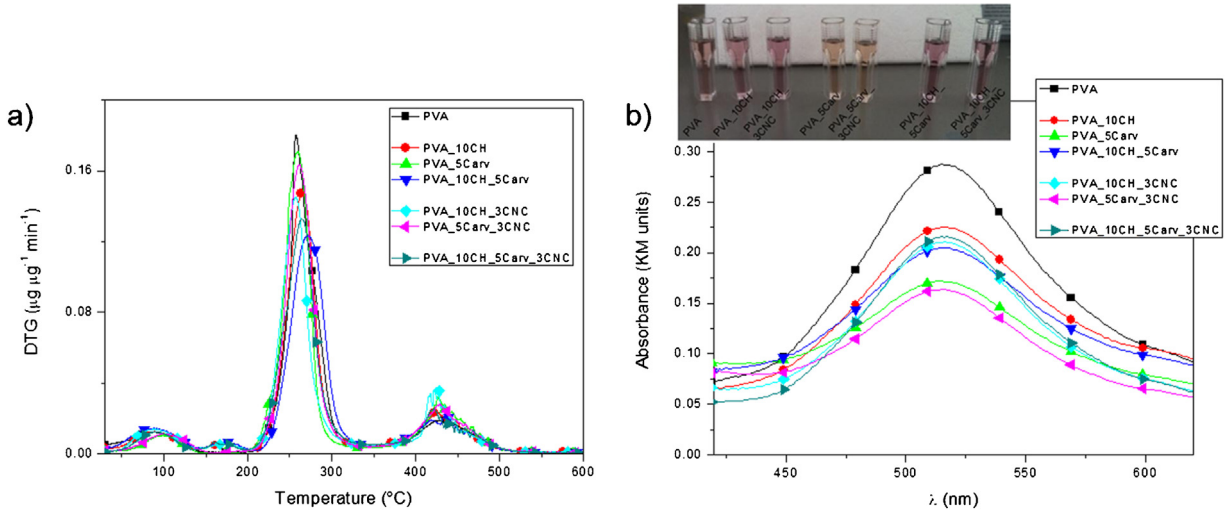

Fig. 5. Thermal properties (a, derivative curves (DTG)) of PVA based films. Antioxidant activities of migrating substances for PVA based formulations immersed directly in the methanol solution for 24 h: monitoring of the absorbance for band at 517 nm (b) and colour variation of the DPPH methanol solution (b, insert).

Table 4
Mechanical properties of PVA based systems.

Formulations	σ_B (MPa)	ε_B (%)	E_{Young} (MPa)
PVA	50.7 ± 6.9	225 ± 30	430 ± 60
PVA_10CH	36.0 ± 9.5	110 ± 25	560 ± 40
PVA_5Carv	57.4 ± 5.3	240 ± 15	400 ± 20
PVA_10CH_5Carv	58.9 ± 7.6	250 ± 35	410 ± 40
PVA_10CH_3CNC	77.0 ± 4.4	215 ± 50	613 ± 62
PVA_5Carv_3CNC	58.7 ± 3.3	250 ± 30	560 ± 80
PVA_10CH_5Carv_3CNC	77.5 ± 12.6	280 ± 25	480 ± 10

Table 5
Radical scavenging activity (RSA) for PVA based systems.

Formulations	DPPH scavenging activity, RSA (%)
PVA	0
PVA_10CH	26.8 ± 0.4
PVA_5Carv	41.9 ± 2.3
PVA_10CH_5Carv	29.0 ± 0.3
PVA_10CH_3CNC	26.3 ± 0.6
PVA_5Carv_3CNC	43.4 ± 0.4
PVA_10CH_5Carv_3CNC	28.3 ± 2.3

due to the loss of the residual acetic acid and adsorbed bound water [53]. The main degradation step of PVA film centered at around 257 °C was related to removal of residual acetate groups due to the incomplete hydrolysis of PVA that remain in the chains [26,56]. The presence of chitosan increase the thermal stability of PVA [49] (PVA: T_{max} = 257 °C and PVA_10CH: T_{max} = 265 °C) while the presence of carvacrol and/or CNC did not affect the thermal stability of PVA and PVA_10CH based formulations (Table 3). Finally, the degradation step centered at around 430 °C (Fig. 5a) was attributed to the elimination of residual acetate groups and the cyclization reaction [57], and it was not influenced by the presence of different components added to PVA matrix.

The effect of chitosan, carvacrol and cellulose nanocrystals in PVA matrix was also investigated in terms of mechanical responses by means of tensile tests and the results are summarized in Table 4. PVA film showed tensile strength of (σ_B = 50.7 ± 6.9) MPa, an elongation at break of (ε_B = 225 ± 30) % and a Young's modulus of (E_{Young} = 430 ± 60) MPa. As previously reported in literature, the addition of 10%wt of chitosan in PVA matrix induced a reduction in terms of tensile strength and elongation at break values for PVA_10CH film (σ_B = 36.0 ± 9.5 MPa and ε_B = 110 ± 25%) respect to neat PVA film [49,58], although the presence of chitosan was able to induce a slight increase of Young's modulus for PVA_10CH film (560 ± 40) MPa respect to PVA film [20]. Moreover, although the presence of 5%wt of carvacrol, used as antimicrobial additive in this research activity, did not affect the mechanical response of PVA matrix. Moreover, although the presence of 5%wt of carvacrol, used as antimicrobial additive in this research activity, did not affect the mechanical response of PVA matrix, its effect was evident when added to PVA_10CH blend inducing an evident increase in tensile strength and elongation at break.

On the other hand, CNC added at 3%wt into PVA and PVA_10CH, were able to increase the tensile strength and the Young's modulus values and this effect was more evident for the formulations that contained also the chitosan (PVA_10CH_3CNC and PVA_10CH_5Carv_3CNC).

PVA_10CH_3CNC and PVA_10CH_5Carv_3CNC based formulations showed, in fact, the highest values of tensile strength ((77.0 ± 4.4) MPa and (77.5 ± 12.6) MPa, respectively), an evident increase in the E_{Young} values and, at the same time, maintained the good elongation at break of PVA matrix that resulted also enhanced for PVA_10CH_5Carv_3CNC (280%). This behavior highlighted the synergic interaction between cellulosic nanofiller and the polymer chains, while cellulose nanocrystals resulted as an efficient load transfer tool [20]. In conclusion, PVA_10CH_5Carv_3CNC resulted the best formulation in terms of elastic and plastic mechanical responses, of fundamental importance for the final application in the packaging sector.

3.4. Antiradical activity, overall migration test and moisture content of PVA and PVA_CH based systems

In food packaging applications, antiradical activities represent important properties requested to a polymeric system that could be in direct contact with food products. Moreover, the moisture content that could be absorbed by the food packaging from the external and/or internal environmental, can determined some deterioration of food products. The continue demand of active and intelligent food packaging systems had promoted the development and use of active principles into packaging devices. The antioxidant release measurements were evaluated by DPPH method.

The test was based on the scavenging of the free radical of carvacrol, releasing from the films during the test. This study is an indirect method used to evaluate the antiradical activity of the produced films. In this work, carvacrol, was selected as active principle to induce the radical scavenging activity on food products and the antioxidant performance of the PVA and PVA_10CH based systems containing the active agent, was evaluated by the scavenging activity of methanol migration extracts against the DPPH radical.

Table 5 and Fig. 5b summarize the antioxidant behavior of migrating substances in methanol for 24 h for different produced films. PVA neat film was selected as control. The presence of carvacrol in PVA and in PVA_10CH based films reduced the DPPH radicals to a yellow-colored compound (see Fig. 5b insert), this behavior was due to the reaction extent relies on the hydrogen-donating ability of the antioxidant principles [59,60]. Specifically, this effect was more visible for PVA_5Carv and PVA_5Carv_3CNC (Fig. 5b, insert). Moreover, the incorporation of 10% wt of chitosan or 5% wt of carvacrol determined a decrease of absorption values at 517 nm (Fig. 5b) and consequently RSA value increased (Table 5), this phenomenon highlighted that chitosan and carvacrol act as antioxidant agents. The presence of chitosan in PVA matrix determined in PVA_10CH film a reduction of absorption values from 0.2861 to 0.2111 and the radical scavenging activity value increased until to 26.8% for PVA_10CH film in accordance to the literature [60–62]. The radical scavenging mechanism of chitosan was due to the reaction of the residual free amino (NH_2) groups with free radicals forming stable macromolecule radicals, afterwards NH_2 groups form ammonium (NH_3^+) groups by absorbing the hydrogen ions from the solution [63]. Moreover, the presence of carvacrol in PVA based films induced an appreciable antioxidant activity, and the RSA value was increased till 41.9% and 43.4%, for PVA_5Carv and PVA_5Carv_3CNC films, respectively. The presence of 3% wt CNC in PVA_10CH_3CNC and in PVA_5Carv_3CNC film did not modify the RSA values respect PVA_10CH and PVA_5Carv, as expected (Table 5). Finally, the combination of chitosan and carvacrol in PVA_10CH_5Carv and in PVA_10CH_5Carv_3CNC multifunctional films determined a slight reduction of RSA respect to PVA_5Carv and PVA_5Carv_3CNC films (Table 5); this phenomenon could be related to the presence of 1%wt of acetic acid used during the solvent process of chitosan that could reduce and/or inhibit the antioxidant activity of carvacrol.

Overall migration test with food simulants were shown in Fig. 6. The test in accordance with the Commission Regulation EU 10/2011 [38] permitted to simulate and to evaluate the polymeric material that could be migrate from the packaging to the foodstuff. The analysis was performed by using two different simulants, ethanol 10% (v/v) and isooctane (A and substitutive D2, respectively). The overall

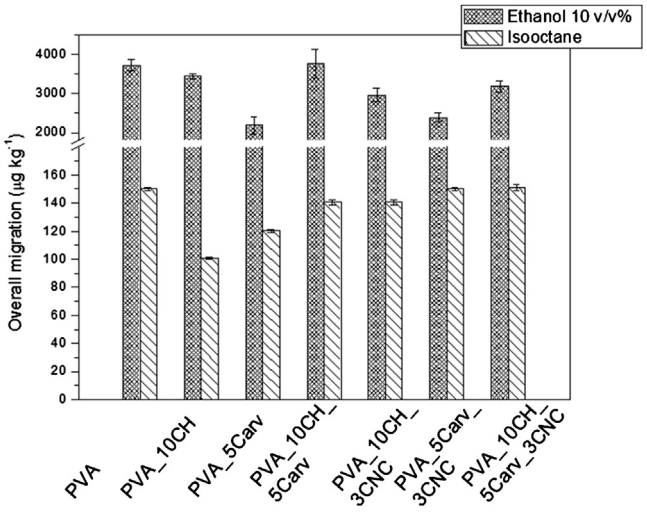

Fig. 6. Overall migration in ethanol 10 (v/v)% and isooctane of PVA based formulations.

Table 6
Moisture content (*MC*) of PVA based systems.

Formulations	MC (%)	
	1th week	5th week
PVA	6.3 ± 0.2	6.4 ± 0.2
PVA_10CH	6.2 ± 0.1	5.6 ± 0.2
PVA_5Carv	5.3 ± 0.1	4.6 ± 0.1
PVA_10CH_5Carv	5.2 ± 0.2	4.2 ± 0.3
PVA_10CH_3CNC	5.2 ± 0.3	3.7 ± 0.1
PVA_5Carv_3CNC	5.3 ± 0.2	5.2 ± 0.1
PVA_10CH_5Carv_3CNC	5.6 ± 0.1	3.9 ± 0.3

migration levels using both food simulants for all the studied formulations were below the migration permitted limits, 60 mg kg^{-1} of simulant, established by the current European legislation. The analysis permitted to demonstrate the possible practical application of the produced films in the food packaging field. Regarding the stimulant A and after 10 days of incubation at 40 °C, PVA migrated value was around 3.719 mg kg^{-1} and the maximum migrated value 3.758 mg kg^{-1} was registered for PVA_10CH_5Carv. The high values of PVA based systems in contact with simulant A were due to the hydrophilic nature and to the high affinity with polar solvent as water of polymer matrix chosen for this work [20,42]. The maximum migrated values (0.150 mg kg^{-1} simulant) was observed for PVA, PVA_5Carv_3CNC, PVA_10CH_5Carv_3CNC after 2 days at 20 °C in isooctane. However, all the migration values of PVA based films were well below the overall migration legislative limits, confirming the possible use of proposed formulations for food-packaging.

Table 6 shows the moisture content (MC) of PVA and PVA_CH based films after 1 and 5 storage weeks at 53% RH and 25 °C. The test permits to evaluate the moisture content that the different produced films could be adsorbed in the selected condition of temperature and humidity. The MC of the PVA film was (6.3 ± 0.2) % and (6.4 ± 0.2) % after 1 or 5 weeks of storage, respectively. Data indicate that the equilibrium was reached after only 1 week of storage in accordance to the literature [64]. Moreover, the PVA film shown higher values than the PVA and PVA_10CH based films, this behavior was due to the higher hydrophilic nature of PVA [42,48]. The presence of carvacrol determined a reduction of moisture content values in PVA and PVA_10CH based films this effect was related to the hydrophobic nature of selected active principle [65,66]. The MC of PVA_5Carv film was (5.3 ± 0.1) % and (4.6 ± 0.1) % after 1 or 5 weeks of storage, respectively. The presence of CNC in PVA_10CH_3CNC film determined a reduction of moisture content respect to PVA_10CH system, this effect can be due to the barrier effect induced by the addition of CNC in thermoplastic matrices [20]. After 5 weeks of storage, the MC values for all different produced formulations tended to reduce respect to the values obtained after 1 week of storage (Table 6), this behaviour was ascribed to some aging phenomena of the selected materials in accordance to the literature [20].

3.5. Antibacterial properties of PVA and PVA_CH based systems

The antibacterial test of PVA and PVA_CH based systems were conducted respect to four bacterial plant pathogens, belonging to three different kinds *Genera*, *Pectobacterium*, *Erwinia* and *Xanthomonas,* and the results are summarized in Fig. 7. From tests with *Pectobacterium carotovorum* subsp. *odoriferum* (Pco) emerged the efficacy of cellulose nanocrystals associated with carvacrol in the films, in fact the thesis subjected to this treatment did record a significantly lower bacterial population than the control. The reduction was quantified at 1 log unit in fact at the time 12 h in the positive control was measured the population was 5.82×10^7 CFU/mL than determined in PVA_5Carv_3CNC thesis, in which the population was present at a concentration equal to 1.95×10^6 CFU/mL. Good results were similarly recorded by using all films containing cellulose nanocrystals; in fact these, compared with the respective waived cellulose nanocrystals, determined a lower bacterial population values (Fig. 7a).

On the contrary, the tests with the strain of *Erwinia amylovora* (Ea) (Fig. 7b) emerged as the bacterium multiplication was not altered, and the films seems to allow the increasing of its values. Last test taking, 12 h, the results showed a positive control population (1.20×10^7 CFU/mL) significantly lower than that measured in the other thesis. The highest values were measured in the theses characterized by the presence of PVA_5Carv and PVA_10CH_5Carv respectively 4.79×10^7 CFU/mL and 4.94×10^7 CFU/mL. The best results obtained were detected in the films containing only chitosan and the same with CNC, even if Ea populations was significantly higher than the control. Viewing results obtained are noted a reduction of bacterial growth with films containing cellulose nanocrystal, compared to their thesis films that not containing.

The *Xanthomonas* strains belonging to two different species *axonopodis* and *arboricola* respectively provided opposite responses (Fig. 7c and d, respectively). In the case of Xav, the causal agent of tomato bacterial spot, the positive control at the time was 12 h measure a value of 6.15×10^6 CFU/mL, on the contrary, a lower population was registered with PVA_10CH_5Carv film, 1.99×10^5 CFU/mL. Overall, it showed effectiveness in containing Xav growth by about 1 log unit of all the films used except for one containing only chitosan, which was even recorded a significantly higher population for the positive control (9.05×10^6 CFU/mL). The *Xanthomonas arboricola* pv. *pruni* (Xap) gave completely opposite data (Fig. 7d) and answers to what we saw with Xav; in fact in the specific case does not showed a reduction of bacteria rather the theses in which there were the films showed higher values than the control. Significantly lower populations were measured on PVA_5Carv_3CNC, PVA_10CH and PVA_10 CH_5Carv, especially the latter which determined minimum values respectively 8.05×10^7 CFU/mL and 9.80×10^7 CFU/mL [67].

4. Conclusions

Poly(vinyl alcohol) (PVA) and natural chitosan (CH) were combined for the production, by cheap and sustainable solvent casting in water technique, of multifunctional films containing cellulose

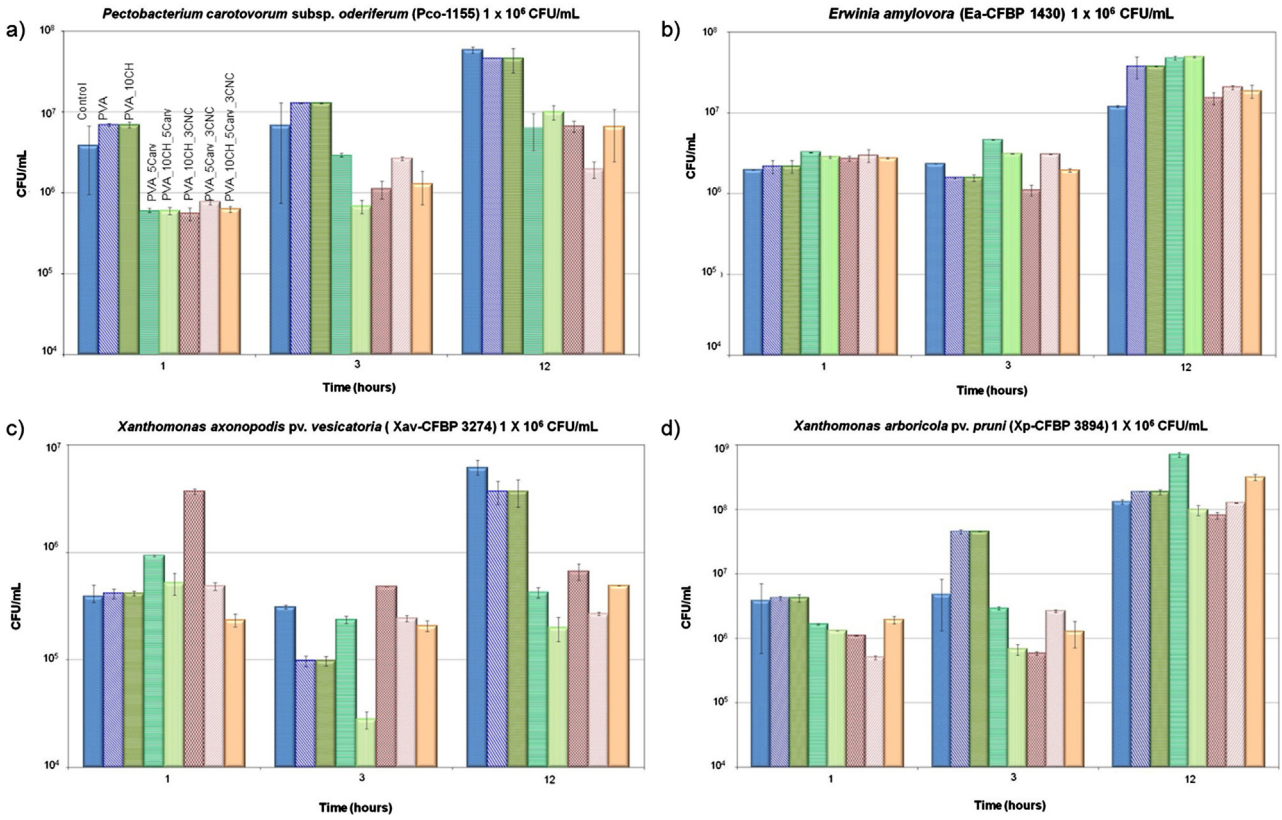

Fig. 7. Antibacterial activities of PVA based formulations respect to *Pectobcterium carotovorum* susp. *odoriferum* (Pco – 1115) (a), *Erwinia amylovora* (Ea – CFBP 1430) (b), *Xanthomonas axonopodis* pv. *vesicatoria* (Xav – CFBP 3274) (c) and *Xanthomonas arboricola* pv. *pruni* (Xap – CFBP 3894) (d) multiplication.

nanocrystals (CNC) extracted from kiwi *Actinidia deliciosa* pruning residues, that were introduced as reinforcement phases also combined with natural carvacrol, here used as active agent. Cellulose nanocrystals were successfully extracted from kiwi pruning shoots, for the first time, by applying an optimize extraction procedure (0.7% wt/v two times of sodium chlorite $NaClO_2$) followed by an hydrolysis step and then combined with carvacrol in novel PVA or PVA_10CH based films for perspective industrial applications. Morphological and optical characteristics, mechanical responses, thermal and migration properties, moisture content and antioxidant and antimicrobial assays were conducted. The morphological analysis underlined that no particular alterations in the PVA and PVA_CH fractured surfaces were induced by the presence of both carvacrol and/or cellulosic nanostructures highlighting the good interaction between the selected additives and the polymer matrices obtained during the film processing. Similarly, optical and colorimetric results, underlined that no particular variations were induced on the transparency and color of PVA and PVA_CH blend that were maintained, after the processing, also when both carvacrol and CNC at 3% wt, were added to the polymer and blend.

Concerning the mechanical and thermal responses, of interest for the final application in industrial sector as food packaging, the results underlined as the combination of active agent and CNC caused a modulation of elastic and plastic mechanical characteristics that was particular evident for PVA_10CH_5Carv_3CNC multifunctional system. However, the typical nucleation phenomenon induced by CNC in thermoplastic matrices and also here reported for PVA based formulations, it was not so evident when CNC were added to PVA_CH since the presence of chitosan, with its amorphous nature, was predominant in the thermal response of produced PVA_CH based formulations.

All the proposed formulations underlined an important antioxidant effect that was particular evident for carvacrol based systems whereas the barrier effect induced by both carvacrol and CNC, was highlighted by moisture content test stressing the effectiveness of the proposed formulations to improve the shelf-life and quality of perishable food products that are, at the same time, able to maintain the migration levels below the permitted limits imposed by the European legislation. Respect to the antibacterial activities of the films here tested, were reasonable to develop few, but original conclusions. Considering the known isolates bacterial plant pathogens tested, only Ea known strain resulted not influenced by different produced formulations. In this case, even with values higher than those obtained in the controls, the best result was recorded by using the PVA_10CH_3CNC film; lightly, by the same film, was affected the Xap multiplication. Respect to the other bacteria tested, it is reasonable to hypothesize a synergistic effect of chitosan, carvacrol and cellulosic additives.

Pco multiplication was remarkably reduced by using PVA_5Carv_3CNC film and by the different combinations in films containing carvacrol and cellulose nanocrystals. Indeed this combination, they resulted able to produce a remarkable reduction also of Xav bacterial population at 12 h by using by using PVA_10CH_5Carv film. In this study was confirmed the possibility to valorize agricultural wastes obtaining precursors for cellulose nanocrystals useful to develop biodegradable films for active packaging [20,63].

Taking into account the losses caused by these bacteria on relevant fresh fruit and vegetable food products, also during their commercialization, the here proposed research activities deserve to be furtherly improved to develop others sustainable films useful to contrast dangerous pests and able to prolong the shelf life of relevant agri-food productions.

Acknowledgment

The Authors acknowledge Dr. Alessandro Di Michele for XRD analysis.

References

[1] F. Luzi, E. Fortunati, A. Jiménez, D. Puglia, D. Pezzolla, G. Gigliotti, J.M. Kenny, A. Chiralt, L. Torre, Production and characterization of PLA_PBS biodegradable blends reinforced with cellulose nanocrystals extracted from hemp fibres, Ind. Crops Prod. 93 (2016) 276–289.
[2] N. Peelman, P. Ragaert, B. De Meulenaer, D. Adons, R. Peeters, L. Cardon, F. Van Impe, F. Devlieghere, Application of bioplastics for food packaging, Trends Food Sci. Technol. 32 (2013) 128–141.
[3] Y. Pan, M. Farmahini-Farahani, P. O'Hearn, H. Xiao, H. Ocampo, An overview of bio-based polymers for packaging materials, J. Bioresour. Bioprod. 1 (2016) 106–113.
[4] E. Fortunati, W. Yang, F. Luzi, J.M. Kenny, L. Torre, D. Puglia, Lignocellulosic nanostructures as reinforcement in extruded and solvent casted polymeric nanocomposites: an overview, Eur. Polym. J. 80 (2016) 295–316.
[5] M.J. Khalaj, H. Ahmadi, R. Lesankhosh, G. Khalaj, Study of physical and mechanical properties of polypropylene nanocomposites for food packaging application: nano-clay modified with iron nanoparticles, Trends Food Sci. Technol. 51 (2016) 41–48.
[6] Z. Qazanfarzadeh, M. Kadivar, Properties of whey protein isolate nanocomposite films reinforced with nanocellulose isolated from oat husk, Int. J. Biol. Macromol. 91 (2016) 1134–1140.
[7] F.G. Calvo-Flores, J.A. Dobado, Lignin as renewable raw material, Chem. Sus. Chem. 3 (2010) 1227–1235.
[8] Y. Habibi, Key advances in the chemical modification of nanocelluloses, Chem. Soc. Rev 43 (2014) 1519–1542.
[9] A. Pakarinen, J. Zhang, T. Brock, P. Maijala, L. Viikari, Enzymatic accessibility of fiber hemp is enhanced by enzymatic or chemical removal of pectin, Bioresour. Technol. 107 (2012) 275–281.
[10] M. Grella, M. Manzone, F. Gioelli, F.P. Balsari, J. Agric. Eng. Res. 44 (2013) 14.
[11] R. Testolin, A.R. Ferguson, New Zeal. J. Crop Hort. Sci. 37 (2009) 1–32.
[12] G. Nemli, H. Kırcı, B. Serdar, N. Ay, Suitability of kiwi (*Actinidia chinensis* Planch.) prunings for particleboard manufacturing, Ind. Crops Prod. 17 (2003) 39–46.
[13] A. Gencer, The utilization of kiwi (Actinidia deliciosa) pruning waste for kraft paper production and the effect of the bark on paper properties Drewno, Prace Naukowe. Doniesienia. Komunikaty 58 (2015) 194.
[14] N. Lin, A. Dufresne, Nanocellulose in biomedicine: current status and future prospect, Eur. Polym. J. 59 (2014) 302–325.
[15] E.M. Fernandes, R.A. Pires, J.F. Mano, R.L. Reis, Bionanocomposites from lignocellulosic resources: properties, applications and future trends for their use in the biomedical field, Prog. Polym. Sci. 38 (2013) 1415–1441.
[16] M.A. Saïd Azizi Samir, F. Alloin, M. Paillet, A. Dufresne, Tangling effect in fibrillated cellulose reinforced nanocomposites, Macromolecules 37 (2004) 4313–4316.
[17] H.A. Silvério, W.P.F. Neto, N.O. Dantas, D. Pasquini, Extraction and characterization of cellulose nanocrystals from corncob for application as reinforcing agent in nanocomposites, Ind. Crops Prod. 44 (2013) 427–436.
[18] M. Matos Ruiz, J.Y. Cavaillé, A. Dufresne, J.F. Gérard, C. Graillat, Processing and characterization of new thermoset nanocomposites based on cellulose whiskers, Compos. Interfaces 7 (2000) 117–131.
[19] Y. Nakano, Y. Bin, M. Bando, T. Nakashima, T. Okuno, H. Kurosu, M. Matsuo, Structure and Mechanical Properties of Chitosan/poly (vinyl Alcohol) Blend Films, Wiley Online Library, 2007, pp. 63–81.
[20] E. Fortunati, P. Benincasa, G.M. Balestra, F. Luzi, A. Mazzaglia, D. Del Buono, D. Puglia, L. Torre, Revalorization of barley straw and husk as precursors for cellulose nanocrystals extraction and their effect on PVA_CH nanocomposites, Ind. Crops Prod. 92 (2016) 201–217.
[21] M. Pereda, A.G. Ponce, N.E. Marcovich, R.A. Ruseckaite, J.F. Martucci, Chitosan-gelatin composites and bi-layer films with potential antimicrobial activity, Food Hydrocolloids 25 (2011) 1372–1381.
[22] K.W. Kim, B.J. Min, Y.T. Kim, R.M. Kimmel, K. Cooksey, S.I. Park, Antimicrobial activity against foodborne pathogens of chitosan biopolymer films of different molecular weights, LWT-Food Sci. Technol. 44 (2011) 565–569.
[23] M.S. Benhabiles, R. Salah, H. Lounici, N. Drouiche, M.F.A. Goosen, N. Mameri, Antibacterial activity of chitin, chitosan and its oligomers prepared from shrimp shell waste, Food Hydrocolloids 29 (2012) 48–56.
[24] S.Y. Sung, L.T. Sin, T.T. Tee, S.T. Bee, A.R. Rahmat, W. Rahman, A.C. Tan, M. Vikhraman, Antimicrobial agents for food packaging applications, Trends Food Sci. Tech. 33 (2013) 110–123.
[25] E. Fortunati, F. Luzi, L. Dugo, C. Fanali, G. Tripodo, L. Santi, J.M. Kenny, L. Torre, R. Bernini, Effect of hydroxytyrosol methyl carbonate on the thermal, migration and antioxidant properties of PVA-based films for active food packaging, Polym. Int. 65 (2016) 872–882.
[26] E. Fortunati, F. Luzi, C. Fanali, L. Dugo, M.G. Belluomo, L. Torre, J.M. Kenny, L. Santi, R. Bernini, Hydroxytyrosol as active ingredient in poly(vinyl alcohol) films for food packaging applications, J. Renewable Mater. 5 (2017) 81–95.
[27] R. Sweetie Kanatt, M.S. Rao, S.P. Chawla, A. Sharma, Active chitosan–polyvinyl alcohol films with natural extracts, Food Hydrocolloids 29 (2012) 290–297.
[28] N. Burgos, I. Armentano, E. Fortunati, F. Dominici, F. Luzi, S. Fiori, F. Cristofaro, L. Visai, A. Jiménez, J.M. Kenny, Functional properties of plasticized bio-based poly (lactic acid) _poly (hydroxybutyrate)(PLA_PHB) films for active food packaging, Food Bioprocess Technol. (2017) 1–11.
[29] G. Yuan, H. Lv, B. Yang, X. Chen, H. Sun, Physical properties, antioxidant and antimicrobial activity of chitosan films containing carvacrol and pomegranate peel extract, Molecules 20 (2015) 11034–11045.
[30] M.A. López-Mata, S. Ruiz-Cruz, N.P. Silva-Beltrán, J.D.J. Ornelas-Paz, P.B. Zamudio-Flores, S.E. Burruel-Ibarra, Physicochemical, antimicrobial and antioxidant properties of chitosan films incorporated with carvacrol, Molecules 18 (2013) 13735–13753.
[31] Z.E. Suntres, J. Coccimiglio, M. Alipour, Crit. Rev. Food Sci. Nutr. 55 (2015) 304–318.
[32] E. Fortunati, F. Luzi, D. Puglia, R. Petrucci, J.M. Kenny, J.M.L. Torre, Processing of PLA nanocomposites with cellulose nanocrystals extracted from *Posidonia oceanica* waste: innovative reuse of coastal plant, Ind. Crops Prod. 67 (2015) 439–447.
[33] E. Fortunati, F. Luzi, D. Puglia, F. Dominici, C. Santulli, J.M. Kenny, L. Torre, Investigation of thermo-mechanical, chemical and degradative properties of PLA-limonene films reinforced with cellulose nanocrystals extracted from *Phormium tenax* leaves, Eur. Polym. J. 56 (2014) 77–91.
[34] E.D. Cranston, D.G. Gray, Morphological and optical characterization of polyelectrolyte multilayers incorporating nanocrystalline cellulose, Biomacromolecules 7 (2006) 2522–2530.
[35] E. Fortunati, F. Luzi, A. Jiménez, D.A. Gopakumar, D. Puglia, S. Thomas, S.J.M. Kenny, A. Chiralt, L. Torre, Revalorization of sunflower stalks as novel sources of cellulose nanofibrils and nanocrystals and their effect on wheat gluten bionanocomposite properties, Carbohydr. Polym. 149 (2016) 357–368.
[36] M. Roohani, Y. Habibi, N.M. Belgacem, G. Ebrahim, A.N. Karimi, A. Dufresne, Cellulose whiskers reinforced polyvinyl alcohol copolymers nanocomposites, Eur. Polym. J. 44 (2008) 2489–2498.
[37] Y. Byun, Y.T. Kim, S. Whiteside, Characterization of an antioxidant polylactic acid (PLA) film prepared with α-tocopherol, BHT and polyethylene glycol using film cast extruder, J. Food Eng. 100 (2010) 239–244.
[38] C. European, J. Off. Eur. Commun. 50 (2011) 1–89.
[39] B. Ma, M.E. Hibbing, H.S. Kim, R.M. Reedy, I. Yedidia, J. Breuer, J. Breuer, D. Glasner, N.T. Perna, A. Kelman, Host range and molecular phylogenies of the soft rot enterobacterial genera Pectobacterium and Dickeya, Phytopathology 97 (2007) 1150–1163.
[40] European and Mediterranena Plant Protection Organization, EPPO, www.eppo.int.
[41] M. Kennedy, D. List, Y. Lu, L.Y. Foo, A. Robertson, R.H. Newman, G. Fenton, Kiwifruit Waste and Novel Products Made from Kiwifruit Waste: Uses Composition and Analysis, Springer, 1999, pp. 121–152.
[42] E. Fortunati, D. Puglia, F. Luzi, C. Santulli, J.M. Kenny, L. Torre, Binary PVA bio-nanocomposites containing cellulose nanocrystals extracted from different natural sources: part I, Carbohydr. Polym. 97 (2013) 825–836.
[43] E.N.J. Ford, S.K. Mendon, S.F. Thames, J.W. Rawlins, X-ray diffraction of cotton treated with neutralized vegetable oil-based macromolecular crosslinkers, Cellulose 5 (2010) 10–20.
[44] A. Figen, O. İsmail, S. Pişkin, Devolatilization non-isothermal kinetic analysis of agricultural stalks and application of TG-FT/IR analysis, J. Thermal Anal. Calorim. 107 (2012) 1177–1189.
[45] G. Varhegyi, E. Jakab, F. Till, T. Szekely, Thermogravimetric-mass spectrometric characterization of the thermal decomposition of sunflower stem, Energy Fuels 3 (1989) 755–760.
[46] J. Flandez, I. González Tovar, J. Bayer Resplandis, N.E. El Mansouri, F. Vilaseca Morera, P. Mutjé Pujol, BioResources 7 (2) (2012) 1836–1849.
[47] S. Hajji, A. Chaker, M. Jridi, H. Maalej, K. Jellouli, S. Boufi, M. Nasri, Structural analysis, and antioxidant and antibacterial properties of chitosan-poly (vinyl alcohol) biodegradable films, Environ. Sci. Pollut. Res. 23 (2016) 15310–15320.
[48] G. Kavoosi, B. Nateghpoor, S.M.M. Dadfar, S.M.A. Dadfar, Antioxidant, antifungal, water binding, and mechanical properties of poly (vinyl alcohol) film incorporated with essential oil as a potential wound dressing material, J. Appl. Polym. Sci. 131 (2014).
[49] J. Bonilla, E. Fortunati, L. Atarés, A. Chiralt, J.M. Kenny, Physical, structural and antimicrobial properties of poly vinyl alcohol-chitosan biodegradable films, Food Hydrocolloids 3 (2014) 463–470.
[50] E.M. Abdelrazek, I.S. Elashmawi, S. Labeeb, Chitosan filler effects on the experimental characterization, spectroscopic investigation and thermal studies of PVA/PVP blend films, Physica B: Condens. Matter 405 (2010) 2021–2027.
[51] S. Wang, M.F. Marcone, S. Barbut, L.T. Lim, Fortification of dietary biopolymers-based packaging material with bioactive plant extracts, Food Res. Int. 49 (2012) 80–91.
[52] M. Mahy, L. Eycken, A. Oosterlinck, Evaluation of uniform color spaces developed after the adoption of CIELAB and CIELUV, Color Res. Appl. 19 (1994) 105–121.
[53] J. Bonilla, E. Fortunati, L. Atares, A. Chiralt, J.M. Kenny, Physical, structural and antimicrobial properties of poly vinyl alcohol-chitosan biodegradable films, Food Hydrocolloids 35 (2014) 463–470.
[54] E. Fortunati, M. Peltzer, I. Armentano, L. Torre, A. Jimenez, J.M. Kenny, Effects of modified cellulose nanocrystals on the barrier and migration properties of PLA nano-biocomposites, Carbohydr. Polym. 90 (2012) 948–956.
[55] K. Lewandowska, Miscibility and thermal stability of poly (vinyl alcohol)/chitosan mixtures, Thermochim. Acta 493 (2009) 42–48.

[56] H. Lu, C.A. Wilkie, M. Ding, L. Song, Thermal properties and flammability performance of poly (vinyl alcohol)/α-zirconium phosphate nanocomposites, Polym. Degrad. Stabil. 96 (2011) 885–891.
[57] Z. Peng, L.X. Kong, A thermal degradation mechanism of polyvinyl alcohol/silica nanocomposites, Polym. Degrad. Stabil. 92 (2007) 1061–1071.
[58] S.B. Bahrami, S.S. Kordestani, H. Mirzadeh, P. Mansoori, Poly (vinyl alcohol)-chitosan blends: preparation, mechanical and physical properties, Iran. Polym. J. 12 (2003) 139–146.
[59] U. Siripatrawan, B.R. Harte, Physical properties and antioxidant activity of an active film from chitosan incorporated with green tea extract, Food Hydrocolloids 24 (2010) 770–775.
[60] W. Yang, J.S. Owczarek, E. Fortunati, M. Kozanecki, A. Mazzaglia, G.M. Balestra, J.M. Kenny, L. Torre, D. Puglia, Antioxidant and antibacterial lignin nanoparticles in polyvinyl alcohol/chitosan films for active packaging, Ind. Crops Prod. 94 (2016) 800–811.
[61] W. Xie, P. Xu, Q. Liu, Antioxidant activity of water-soluble chitosan derivatives, Bioorg. Med. Chem. Lett. 11 (2001) 1699–1701.
[62] K.W. Kim, R.L. Thomas, Antioxidative activity of chitosans with varying molecular weights, Food Chem. 101 (2007) 308–313.
[63] M.T. Yen, J.H. Yang, J.L. Mau, Antioxidant properties of chitosan from crab shells, Carbohydr. Polym. 74 (2008) 840–844.
[64] A. Cano, E. Fortunati, M. Cháfer, J.M. Kenny, A. Chiralt, C. González-Martínez, Properties and ageing behaviour of pea starch films as affected by blend with poly (vinyl alcohol), Food Hydrocolloids 48 (2015) 84–93.
[65] J.F. Rubilar, R.M.S. Cruz, H.D. Silva, A.A. Vicente, I. Khmelinskii, M.C.J. Vieira, Physico-mechanical properties of chitosan films with carvacrol and grape seed extract, Food Eng. 115 (2013) 466–474.
[66] K.M. Zia, S. Tabasum, M. Nasif, N. Sultan, N. Aslam, A. Noreen, M. Zuber, A review on synthesis, properties and applications of natural polymer based carrageenan blends and composites, Int. J. Biol. Macromol. 96 (2016) 282–301.
[67] K.M. Zia, S. Tabasum, M. Nasif, N. Sultan, N. Aslam, A. Noreen, M. Zuber, A review on synthesis, properties and applications of natural polymer based carrageenan blends and composites, Int. J. Biol. Macromol. 96 (2017) 282–301.